LBL-17514
c.2

Lawrence Berkeley Laboratory
UNIVERSITY OF CALIFORNIA

EARTH SCIENCES DIVISION

To be presented at the International Association of Hydrogeologists 17th International Congress, Tuscon, AZ, January 7-12, 1985

EFFECTS OF FRACTURE ROUGHNESS ON FLUID FLOW THROUGH A SINGLE DEFORMABLE FRACTURE

Y.W. Tsang and P.A. Witherspoon

October 1984

TWO-WEEK LOAN COPY
This is a Library Circulating Copy
which may be borrowed for two weeks.

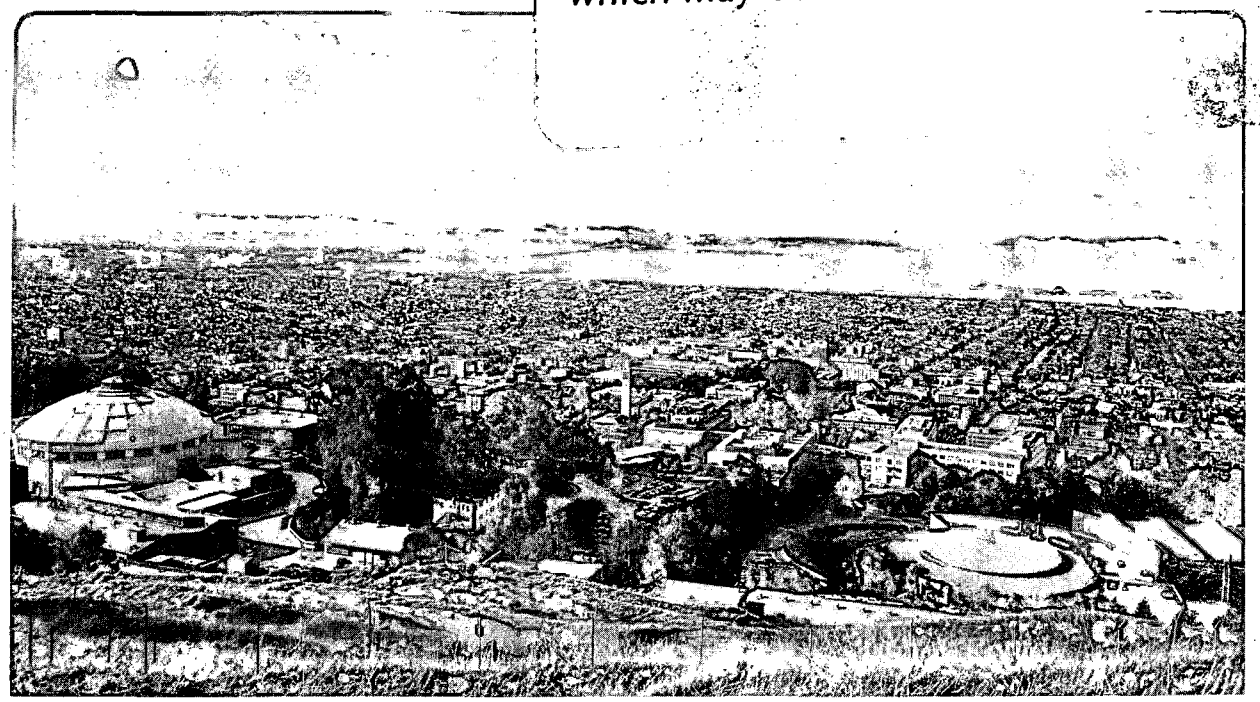

Prepared for the U.S. Department of Energy under Contract DE-AC03-76SF00098

LBL-17514
c.2

DISCLAIMER

This document was prepared as an account of work sponsored by the United States Government. While this document is believed to contain correct information, neither the United States Government nor any agency thereof, nor the Regents of the University of California, nor any of their employees, makes any warranty, express or implied, or assumes any legal responsibility for the accuracy, completeness, or usefulness of any information, apparatus, product, or process disclosed, or represents that its use would not infringe privately owned rights. Reference herein to any specific commercial product, process, or service by its trade name, trademark, manufacturer, or otherwise, does not necessarily constitute or imply its endorsement, recommendation, or favoring by the United States Government or any agency thereof, or the Regents of the University of California. The views and opinions of authors expressed herein do not necessarily state or reflect those of the United States Government or any agency thereof or the Regents of the University of California.

EFFECTS OF FRACTURE ROUGHNESS ON FLUID FLOW THROUGH A SINGLE DEFORMABLE FRACTURE

Y. W. Tsang and P.A. Witherspoon
Earth Sciences Division, Lawrence Berkeley Laboratory
University of California, Berkeley, California 94720

ABSTRACT

The cubic law for fluid flow through a single fracture commonly employed in simulations of fluid flow through a fractured medium assumes the smooth parallel-plate idealization of each fracture. This paper summarizes results of our theoretical investigations on the effects of fracture surface roughness on fluid flow through a single deformable fracture.

A rough fracture may be envisioned as a collection of voids which deform as the fracture closes under stress. Mathematically, the collection of voids can be defined in terms of an aperture density distribution. We constructed a theory to relate the geometrical characteristics of the fracture to its mechanical properties so that an aperture density distribution for the fracture may be derived from fracture stress-strain measurements. A review of available fracture roughness profiles showed that the aperture density distributions of real fractures may take on various shapes: sharply peaked, broad and flat, skewed and peaked toward the large apertures or toward the small apertures. The different shapes give rise to qualitatively different variations of flow rate with normal stress applied to the fracture.

Calculations were first carried out for flow with no tortuosity; then the effect of path tortuosity and connectivity on fluid flow rate were investigated. Our calculations show that for fractures with aperture distribution that is sharply peaked toward the large apertures, the effect of tortuosity is minimal and the fracture remains hydraulically open though its mechanical properties may approach that of an intact rock. On the other hand, when the aperture distribution is dominated by small apertures and when the contact area of the fracture surfaces is above 30%, the effect of tortuosity may depress the fluid flow rate by two or three more orders of magnitude from that predicted by the parallel-plate idealization of the fracture. Thus the applicability of a parallel-plate mean aperture to the description of flow behavior in a rough fracture is limited. Generally, both the aperture distribution and the spatial distribution of these apertures in the fracture are needed to predict the fluid movement in a single deformable fracture.

INTRODUCTION

The movement of fluids through fractured rock masses, and how factors such as stresses affect such movement is of fundamental importance in understanding many earth processes. The recovery of petroleum from fractured reservoirs is a matter of great economic importance. The advent of the problem of isolation of nuclear and toxic wastes in geological formations has introduced a new challenge of seeking out low permeability rock masses where the fluid movement is as close to zero as possible. In all the above, the essential building-block for the understanding of the fluid through the fractured medium is the physical law which governs the flow through one single fracture.

The simplest idealization of a rock fracture is a pair of smooth, parallel plates separated by a uniform distance. The analytic solution to the problem of steady laminar flow of a viscous imcompressible fluid through a pair of parallel plates has been given by many workers [for example, Boussinesq, 1868; Snow, 1965; and Bear, 1972]. The fluid flow rate per unit pressure head difference is proportional to the cube of the parallel plate separation, that is:

$$\frac{Q}{\Delta h} = C\, b_o^{\,3} \quad . \qquad (1)$$

The proportionality constant, C, contains information on the flow field dimensions and fluid properties. If the fracture is represented mathematically by an aperture density distribution, n(b), where n(b)db gives the probability of finding apertures with values between b and (b+db); then the idealized parallel-plate fracture has a n(b) in the form of a delta fraction peaked at b_o. For a rough fracture where the apertures range over different values, the aperture density distribution takes on shapes other than that of a delta function; the actual shape of the n(b) is governed by the roughness characteristics of the fracture in question. Figure 1 shows schematically the difference in n(b) for a pair of parallel plates and a fracture where roughness is present. Equation (1), when applied to flow through a fracture, has often been referred to as the cubic law. Without exception, the state-of-the-art mathematical modeling of flow through a fractured medium (Wang et al, 1983) utilizes this simple parallel-plate idealization of a fracture, assuming that a parallel-plate equivalent aperture b_o can be assigned to the rock fracture.

However, a real fracture in rock masses has rough-walled surfaces, and unlike parallel plates, portions of the fracture may be closed while the rest remains open when the fracture is subject to stress. It is not clear that a physical law which governs the fluid flow through a pair of smooth, parallel plates should be valid for flow through realistic, rough-walled fracture. Indeed, evidences of deviation from the so-called cubic law are found in laboratory experiments of flow in fracture at elevated stress (Engelder and Scholz, 1981; Gale, 1982).

In this paper, we will present the results of our theoretical study on the effect of fracture roughness on the physical law governing the fluid flow in a single fracture. Since the fracture roughness is characterized mathematically by the aperture distribution, n(b), we will first discuss a theory which allows one to deduce n(b) from the rather accessible stress-strain measurements. Then we present our calculations on how the fracture roughness affect the fluid flow through both the aspects of the non-uniform apertures in the fracture and the flow path tortuosity.

GEOMETRICAL CHARACTERIZATION OF FRACTURE ROUGHNESS FROM ELASTIC MEASUREMENTS

We have developed a theory (Tsang and Witherspoon, 1981), from which the mathematical aperture density distribution for a fracture may be deduced from stress-strain measurements. In our approach, we consider a single fracture to be composed of a collection of voids with lengths $2d_j$, defined as the distance between two adjacent areas where the fracture surfaces come into contact. When the normal stress (σ) across the fracture is increased, more areas of the fracture surface come in contact, leading to a decrease in the average crack length. Fig. 2 illustrate the deformation of the voids in a fracture as a function of stress.

Walsh (1965) derived an expression for the effective modulus, E_{eff}, of rock containing a number of voids oriented normal to the direction of loading. As shown in Figure 3, E_{eff} is given by:

$$\frac{1}{E_{eff}} = \frac{1}{E} + \frac{4\pi\langle d^3\rangle}{E\langle u\rangle} \qquad (2)$$

where the half void length cubed, d^3, and the small volume of rock, $u = \Delta x\Delta y\Delta z$, immediately surrounding each void have been averaged over all the voids in the sample and where E is the intrinsic modulus of the rock containing no voids. Equation (2) describes a system of sparse voids where the perturbation of the stress field due to the presence of one void does not influence conditions in the near field of another void, therefore the modulus E of the intact rock appear in the strain energy associated with the cracks (the last term in (2)). However, as shown in Figure 2, a fracture is more accurately represented by a large number of voids in close proximity so that the property of the rock medium in which the voids are situated is better represented by the effective modulus of the fractured rock. We therefore make a plausibility argument and propose that (2) may be modified to:

$$\frac{1}{E_{eff}} = \frac{1}{E} + \frac{4\pi\langle d^3\rangle}{E_{eff}\langle u\rangle} \quad . \qquad (3)$$

For a spatially random number of voids, M, in a fracture of total area A,

$$\langle(2d)^2\rangle M \cong A \qquad (4)$$

and

$$\langle u\rangle = A\Delta z/M \quad . \qquad (5)$$

Equations (3), (4), (5) yield the approximation:

$$\frac{E_{eff}}{E} \cong 1 - \frac{\pi\langle d\rangle}{\Delta Z} \qquad (6)$$

where ΔZ is the thickness around the horizontal fracture over which E_{eff} is applicable. Values of E and E_{eff} may be obtained from the slope of stress-strain data from intact and fractured specimens of the same rock type. Equation (6) gives the physical picture as follows: initially, at small stresses, the average crack length is large and comparable to ΔZ, hence $E_{eff}/E \ll 1$ and the mechanical property of the rock with the single fracture is very soft. Under increasing load, the deformation of the voids causes a decrease in the average crack length which results in a gradual increase of the effective modulus with increasing normal stress according to (6). The average crack length $2\langle d\rangle$ continues to decrease as the voids deform under stress until the term $\pi\langle d\rangle/\Delta Z$ becomes negligibly small compared to 1, at which point the jointed rock will exhibit an effective modulus identical to that of the intact rock. If the voids are assumed to be randomly distributed over the fracture surface, and if the places where the fracture comes into contact has a constant area, a^2, then the number of contact areas, N_c, varies inversely as the average crack length, i.e.,

$$N_c \propto \frac{1}{\langle d\rangle} \quad . \qquad (7)$$

Furthermore, when a fracture closes by Δb from the applied stress, those fractures which have values less than Δb at zero applied stress will become zero, therefore the areas of contact may be related to the fracture aperture distribution n(b) at zero applied stress by

$$N_c(\Delta b) = \frac{A}{a^2}\int_0^{\Delta b} n(b)\,db, \qquad (8)$$

and the aperture distribution function, n(b), can be obtained from the derivative of N_c (Δb). It is evident from (6)-(8) that the aperture density distribution may be derived from the elastic properties of the fracture. However, due to the proportionality relation in (7), N_c and therefore n(b) can only be determined to within some constant multiplier. But if the contact area as a fraction of the total fracture area is known to be ω at a specified stress and deformation Δb, that is,

$$\omega = \frac{\int_0^{\Delta b} n(b)\, db}{\int_0^{\infty} n(b)\, db} , \qquad (9)$$

then the constant multiplier can be determined without ambiguity. Therefore (6) - (9) give the prescription to derive from stress-strain measurements which are generally more experimentally accessible, the geometrical characteristics of the fracture which are less experimentally accessible. Given n(b), the effect of fracture roughness may be incorporated into the fluid flow law. Nenzil and Tracy (1981) proposed a modified cubic law for flow through a rough fracture:

$$\frac{Q}{\Delta h} = C \int_0^{\infty} b^3\, n(b) db = c \langle b^3 \rangle \qquad (10)$$

Eq. (10) corresponds to a physical situation where the apertures of the fracture vary only in the direction normal to the externally imposed hydraulic head, resulting in fluid movement along parallel flow paths involving no tortuosity.

COMPARISON OF NON-TORTUOUS FLOW MODEL WITH DATA

Here we shall consider the application of the above theory to specific cases where experimental measurements are available. Iwai (1976) performed laboratory investigations on the mechanical and hydrological properties of tension fractures in samples of basalt, granite and marble 15 cm in diameter. The normal displacement across the fracture and the change in flow conductivity through the fracture are measured as a function of stress during loading and unloading under normal stresses up to 20 MPa.

Making use of (6) - (9), the mathematical aperture distribution for the rough fracture under zero stress is deduced. With applied stress, the fracture closes and all apertures smaller than the fracture closure Δb will become zero. The new aperture distribution f(b') may be expressed in terms of the distribution at zero stress n(b),

$$f(b') = n(b-\Delta b) \quad . \qquad (11)$$

Equipped with the aperture distributions, the flow as a function of stress is predicted using (10) and compared with experimental data. The theoretical and experimental relationships between flow per unit head and normal stress are compared in Figure 4 for one cycle of loading and unloading on the granite sample. The agreement is good and no curve fitting using adjustable parameters is involved. Recall that the value of ω, the fractional contact area, is required in the derivation of aperture distribution, n(b), from the stress-displacement data. Iwai (1976) estimated ω for both the granite and basalt samples to be between 10 to 20% at the maximum applied stress of 20 MPa. The value 15% was chosen in the calculations involved in Figure 4. Figure 5 shows the effect of the value for ω on the theoretical prediction of flow in the basalt sample.

Since no curve fitting is involved in the handling of the flow data, the good agreement of our theory with experiment such as those shown in Figures 4 and 5 testify to the fact that in spite of several simplifying assumptions, the 'void' model which allow us to start with stress-strain properties of a fracture to arrive at an aperture distribution which characterize the rough fracture, probably contain the essential physics that govern the deformation mechanism in a fractured rock. Our work differs from other works which deal with the flow through a rough fracture (Walsh, 1981; Gangi, 1978) in that we deduce the aperture density distribution from the stress-stain measurements and the other works assume some form of aperture distribution. Our approach of using a collection of voids to characterize the fracture and treating the displacement with stress as the deformation of voids allows the deduction the aperture distribution without actual geometrical measurements.

EFFECT OF TORTUOSITY ON FLUID FLOW

The good agreement, as presented in the previous section, between actual flow measurements and theoretical predictions based on the flow model of (10) where the effect of tortuosity is not included, seems to indicate that the tortuosity of flow paths, which must be present in flow in a real rock fracture, plays a negligible role in affecting the fluid flow rate. However, a systematic study specifically directed at the effect of tortuosity on flow through a fracture show that it is a strong function of the roughness characteristics of the fracture, and for certain aperture distributions, the effect of tortuoisty can be significant.

To calculate quantitatively the effect of tortuosity and connectivity of flow paths on the fluid flow rate, we modeled the variation of fracture apertures by electrical resistances. The method of electrical analog to study groundwater movement in a porous medium is an established technique (for example: Luthin, 1953; Fatt, 1956; Bouwer and Little, 1959). The governing equations for the fluid flow and electrical current are identical, giving rise to one to one correspondence between: (a) the fluid flow rate, Q, and the electrical current, i, (b) the hydraulic head, h, and the electrical potential, V, and (c) the hydraulic conductivity and the electrical conductivity. Parsons (1966) had also applied the technique to an idealized fractured medium, that is, a multiple fracture system. The following study is an application of this numerical technique to the problem of fluid flow through a single fracture with rough surfaces. The applicability of the electrical analog method to the study of flow in a single fracture has been demonstrated in a laboratory study by Sundaram and Frink (1983).

In our calculation, the variation of apertures b in the rough fracture is modeled by N electrical resistors with different resistance values placed on a two-dimensional grid, as shown in Fig. 6a. The resistances take on values $1/b^3$ with the b's obeying the aperture distribution n(b), of the fracture. With applied stress and subsequent fracture closure Δb, the resistors take on the values $1/(b - \Delta b)^3$. It is clear that as fracture contact area increases with applied stress, more and more of these resistances become infinite and thus impassable to the electric current.

The grid size, N, is determined by the size of the asperities in the fracture and the rock sample size. In correlating the resistance R to $1/b^3$, We have assumed that the fracture roughness is such that there exists a typical asperity size, a, which is defined as the length over which the aperture of the fracture remains essentially constant; then a fracture of cross-sectional area A may be represented by a grid consisting of $N = A/a^2$ resistors. The electrical analog of a flow situation described by Equation (10), where tortuosity is absent and fluid movement is along flow paths parallel to the hydraulic head, is a set of resistors connected in parallel, as shown in Fig. 6b. The resistances take on values $1/(b-\Delta b)^3$ consistent with a given aperture distribution, n(b), as described earlier. The current through such a set of resistors in parallel is uniquely determined by the

given n(b), that is, assignment of the same set of resistance values governed by a given n(b) to different positions in the parallel network gives identical calculated current value.

However, when the resistors are placed in a two-dimensional grid as shown in Fig. 6a, the current will vary according to the different spatial placement of the resistance values. The spread in the current values with respect to the different spatial placement of resistances, and the discrepancy between these values and the current value through the same set of resistors all connected in parallel, is then a measure of the effect of tortuosity on the flow rate. For our study, we calculated numerically for a specified n(b), (1) the electrical current, $\bar{i}$, through resistances all connected in parallel, (2) the average current, $\bar{i}$, for eight to sixteen random spatial realizations of the same set of resistances on a two-dimensional grid (that is, if the addresss of the resistors are labeled from 1 through N as shown in Figure 6a, then the different spatial arrangement of the resistors can be obtained by assigning the same set of N resistance values corresponding to N(b) in random order to the N addresses), and (3) the standard deviation, δ , for the currents of the different spatial realizations.

Of the aperture distributions used for this systematic study, some were derived from measurements, others were hypothetical analytical functions. Gentier (1983) had measured the roughness profiles of the surfaces of a natural granite fracture, 12 cm in diameter. The measurements were taken from both the top and bottom of the fracture along ten traces, of which five were in one direction, and the other five in the orthogonal direction. A typical profilometer trace is shown in Fig. 7. The spacing between the top and bottom traces gives the aperture b. Note that the y scale is 12.5 times that of the x scale so that the variation of b is greatly exaggerated. The aperture data for all the ten traces measured were collectively plotted in Figure 8. Note that n(b) takes on a skewed shape, with the long tail toward the large apertures. When the fracture closes by Δb as a result of applied stress, all the apertures smaller than Δb become zero. Mathematically, a new aperture distribution is obtained by truncating the original n(b) (when the fracture surfaces are in point contact under zero applied normal stress) by Δb and translating the remaining plot to the origin as in Equation (11). On Figure 8, truncation of the original n(b) corresponding to fractional contact area, ω, of 15, 25 and 35% are marked. Apart from these n(b)'s that were derived from direct measurements, analytic forms of n(b) were also used in this study.

By reviewing (Tsang & Witherspoon, 1983) over available fracture roughness profiles in sandstone and limestone (Bandis, et al., 1981), we have found that the aperture distribution of a very well-matched fracture (i.e., very little lateral misalignment between identical top and bottom fracture halves) takes on a sharply peaked shape; the aperture distribution of an ill-mated fracture is broad and flat. Therefore a Gaussian function was one of the hypothetical analytic functions assumed for the aperature distribution. Two sets with the same mean aperture, b_o, but with the width parameter differing by an order of magnitude were used to simulate the well-matched fracture (narrow width) and the ill-matched fracture (broad width).

Another analytical function chosen for n(b) was:

$$n(b) = \frac{\beta}{\frac{1}{\beta} - \frac{e^{-\beta b_m}}{\beta} - b_m e^{-\beta b_m}} (b_m - b) e^{-\beta(b_m - b)} . \qquad (12)$$

The distribution is normalized so that the integration of n(b) from b = 0 to the maximum aperture b_m is 1. The distribution for two values of the width parameter $1/\beta$ are shown in Figure 9. Small values of the width parameter correspond to a peaked distribution; the distribution flattens out as the width parameter increases. Note that these distributions are skewed, with the peak near the large

aperture end. The aperture distributions derived from stress-strain measurements in granite and basalt samples, (which we discused earlier in the section on flow without tortuosity) resemble the narrow and peaked aperture distribution in Figure 9.

Currents through sets of electrical resistances whose values are determined by the above three aperture distributions were calculated. The same electrical voltage of 10 volts was assumed for all the calculations, regardless of the spatial arrangement of the resistors or the aperture density distribution. Figure 10 displays the calculated results for the n(b) (shown in Figure 8) derived from fracture surface roughness measurements. The horizontal axis is for N, the number of resistors used to represent the given n(b). The points on the three lower curves denote average current $\bar{i}$ and the vertical bars denote one standard deviation δ. The points on the upper three curves are the calculated currents through a set of resistors connected all in parallel, the electrical analog of fluid flow in the absence of tortuosity. These results show the following:

(a) When the resistors are placed on a two-dimensional grid, the total number of resistors N does not seem to play a crucial role in affecting the average current $\bar{i}$, therefore, a relatively small number of resistors may be used to model flow through a single fracture. In fact, aperture profiles from fracture surface profiles such as the one shown in Fig. 7 confirms that the variation of b along such a trace may be represented by a finite number of resistors.

(b) The avêrage current through a two-dimension grid of resistors is about one order of magnitude smaller than the current through the same set of resistors connected in parallel when the n(b) used corresponds to a fractional contact area of 15%. The reduction of the average current through the two-dimensional grid increases with increasing fracture contact area, giving rise to about two orders of magnitude discrepancy when the fractional contact area is 35%.

(c) The spread in values of current ($\delta/\bar{i}$) arising from different spatial placement of the same set of resistance values increases with increasing fracture closure and contact area.

The observations (a) - (c) also apply to the calculations for the Gaussian aperture distribution and the skewed distribution (Figure 9). Our analysis show that small apertures play a key role in depressing fluid flow when one moves from a flow geometry which excludes tortuosity to the actual two-dimensional flow in a rough fracture. Hence the influence of tortuosity is largest when the fracture roughness consists of a large fraction of small apertures, that is, when the aperture distribution is skewed and peaked at small apertures (similar to that in Figure 8 at zero applied stress). Conversely, the influence of tortuosity is smallest when the distribution is sharply peaked at large apertures with a long tail in the small apertures such as that shown in Fig. 9. When the fracture is subject to increasing normal stress, the fraction of zero apertures invariably becomes large regardless of the shape of the aperture distribution at zero stress and the effect of tortuoisty of flow paths become important.

The effect of tortuosity and connectivity of flow paths may be considered negligible when the average current derived from a two-dimensional grid of resistors differs only slightly from that of a one-dimensional array of resistors in parallel, and when the spread of the current values due to different spatial variation of apertures is small. For fractures with sharply peaked aperture distributions (characteristic of very well-matched fractures), the above conditions are met for contact area of less than 14% if the distribution is Gaussian, and for contact area up to 26% if the distribution is skewed toward the large aperture. This might account for the very good agreement with data for granite and basalt which we obtained earlier when a flow model which neglects tortuosity was used. The

contact area there at the maximum applied stress of 20 MPa was between 10-20%, and the aperture distribution derived from those stress-strain data resembled that of the peaked skewed distribution as shown in Figure 9.

In cases where the effect of tortuosity and connectivity of flow paths is small, prediction of fluid flow through the rough fracture only requires the input of the aperture density distribution, which can be obtained from the stress-strain measurements of the fracture, as we showed earlier. Where the effect of tortuosity and connectivity is not negligible, then the knowledge of the actual spatial arrangement of the apertures is needed. Short of knowing the actual spatial arrangement of the apertures, the approach used in this investigation, which is to calculate a statistical average of the currents for different random spatial placement of the same set of apertures can still provide an estimate of the range of flow rates within which an actual measurement may fall.

CONCLUSION

Our investigation show that only at low applied stress, when the fracture is essentially open, is the parallel-plate approximation for a fracture adequate in the description of fluid flow through it. As the contact area between the fracture surfaces increases with stress, the roughness in the fracture surface cease to be mere perturbation on a mean parallel-plate aperture, rather, the aperture distribution is needed. We have shown that the stress strain measurements of the jointed rock afford a way to deduce the aperture distribution.

In addition to this effect of variable apertures, when the contact area of the fracture surface is greater than 30%, the fluid flow rate can be two or more orders of magnitude smaller than that predicted by a flow model which does not include tortuosity. Measurements by Bandis et al., (1983) on models of many sandstone and limestone samples show that the contact area is approximately in the range of 40-70% at an applied stress of 30 MPa.

The conclusion that tortuosity depresses fluid flow in a single fracture may appear to be intuitively obvious, yet its impact on the results of numerical modeling in the field of fracture hydrology is non-trivial. Parallel-plate idealization of each rock fracture, the standard assumption in the state-of-the-art numerical modeling of permeability for a fractured medium [Wang et al, 1983], implies that both the fracture roughness and flow tortuosity play no role in affecting the fluid movement. Our results call attention to the fact that perhaps the several orders of magnitude correction in flow rate due to roughness and tortuosity should not be overlooked. The field experiment of Abelin et al (1983) on a single fracture showed that the equivalent fracture aperture derived from the constant head permeability measurement was many orders of magnitude smaller than that derived from the tracer migration measurement. The equivalent apertures derived from these two different measurements should be identical if the parallel-plate description of the fracture were valid. However, if roughness were present, then the permeability measurement would be controlled by the small apertures and therefore greatly affected by tortuosity, whereas the tracer test would measure the 'volumetric' flow and not affected by tortuosity. These field data therefore support our claim that the equivalent parallel-plate aperture alone is not sufficient in the description of fluid flow in a single fracture.

ACKNOWLEDGEMENT

This work was supported by the Director, Office of Energy Research Office of Basic Energy Science, of the U.S. Department of Energy under Contract No. DE-AC03-76SF00098.

NOTATION

a	typical asperity size, L
A	fracture cross-section area, L^2
b	fracture aperture, L
b_m	maximum aperture, L
b_o	aperture at peak of aperture distribution, L
d	crack length, L
C	constant in cubic flow law, $(LT)^{-1}$
E	Young's modulus for rock, M/LT^2
E_{eff}	effective Young's modulus for jointed rock M/Lt^2
$\bar{i}$	average current (ampere)
h	hydralic head, L
$n(b)db$	aperture distribution (dimensionless)
$f(b')db'$	aperture distribution (dimensionless)
N	total number of resistors on the two-dimensional grid
N_c	number of areas of contact in fracture
Q	fluid flow rate, L^3/T
u	volume enclosing one crack, L^3
Δb	fracture closure, L
β	inverse width parameter in the skewed distribution of fracture aperture, L^{-1}
σ	standard deviation of current (ampere)
σ	stress normal to fracture M/LT^2
ω	fractional contact area

REFERENCES

Abelin, H., J. Gidlund, I. Neretnieks, 1983, Migration experiments in a single fracture in the Stripa granite. Preliminary results. Proceedings of the workshop on Geological disposal of radioactive waste in situ experiments in granite, Stockham, Sweden, Published by OECD (Organisation for Economic Co-operation and Development 97575 Paris Cedex 16, France.

Bandis, S., A. C. Lumsden and N. R. Barton, 1983, Experimental studies of scale effects on the shear behavior of rock joints, Int. J. Rock Mech. Min. Sci. 18, 1-21.

Bear, J., 1972, Dynamics of Fluids in Porous Media, Elsevier, New York,

Boussinesq, J., 1868, Memoire sur l'influence des frottments dans les mouvements reguliers des fluids, J. Liouville, 13, 377-424, .

Bouwer, H. and W.C. Little, 1959, An unifying numerical solution for two-dimensional steady flow problems in porous media with an electrical resistance network, Soil Sci. Soc. Amer. Proc., 23, 91-96.

Engelder, T. and C. H. Scholz, 1981, Fluid flow along very smooth joints at effective pressure up to 200 megapascals, Geophysical Monograph 24, 147-152, Washington, D. C.

Fatt, I., 1956, The Network Model of Porous Media II and III, Trans. AIME 207, 160-181.

Gale, J. E., 1982, The effects of fracture type (induced versus natural) on the stress-fracture closure-fracture permeability relationships, proceedings, at 23rd Symposium on Rock Mechanics, The University of California, Berkeley, California.

Gangi, A. F., 1978, Variation of whole and fractured porous rock permeability with confining pressure, Int. J. Rock Mech. Min. Sci., 15, 249-257.

Gentier, S., 1983, BRGM et Université d' Orléans, personal communication.

Iwai, K., 1976, Fundamental studies of the fluid flow through a single fracture, Ph.D. Thesis, University of California, Berkeley

Kranz, R. L., A. D. Frankel, T, Engelder, and C. H. Scholz, 1979, The permeability of whole and jointed Barre granite, Int. J. Rock, Mech. Min. Sci., 16, 225-234.

Luthin, J.N., 1953, An electrical resistance network for solving drainage problems, Soil Sci., 75, 259-274.

Neuzil, C. E., and J. V. Tracy, 1981, Flow through fractures, Water Resour. Res., 17, 191-199.

Parsons, R.W., 1966, Permeability of idealized fractured rock, Soc. of Petroleum Eng. J., 126-136.

Snow, D.T., 1965, A Parallel plate model of fractured permeable media, Ph.D. Thesis, Univ. of Calif, Berkeley.

Sundaram, P.N. and D. Frink, 1983, Electrical analogy of hydraulic flow through rock fractures, Geotech. Testing J. Vol. 6 No. 1 pp.3-9.

Tsang, Y. W. and P. A. Witherspoon, 1981, Hydromechanical behavior of a deformable rock fracture subject to normal stress, J. Geophys. Res., 86(B10), 9287-9298.

Tsang, Y. W. and P. A. Witherspoon, 1983, The dependence of fracture mechanical and fluid properties on fracture roughness and sample size, J. Geophys. Res., 88(B3), 2359-2366.

Walsh, J. B., 1981, Effect of pore pressure and confining pressure on fracture permeability, Int. J. Rock Mech. Min. Sci., 18, 429-435.

Wang, J.S.Y., C.F. Tsang, and R.A. Sterbentz, 1983, The state of the art of numerical modeling of thermohydrologic Flow in fracture rock masses, Environ. Geol. 4, 133-199.

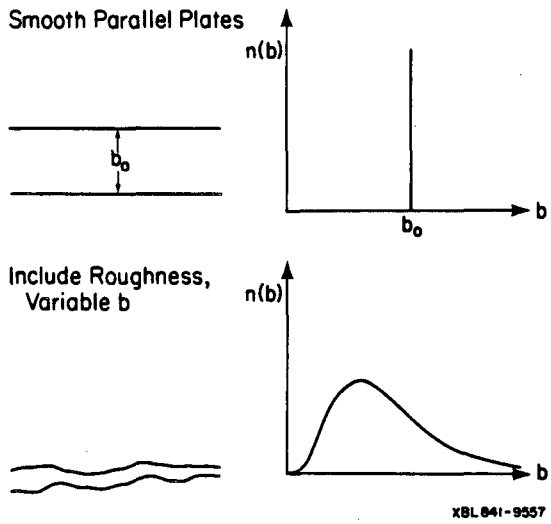

Figure 1. Schematic aperture distributions for an idealized smooth fracture and a rough fracture.

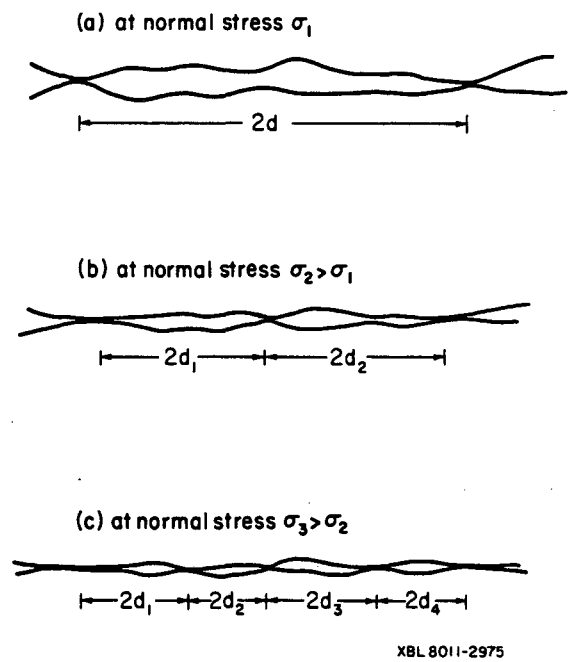

Figure 2. Deformation of 'voids' in a sequence of increasing normal stress.

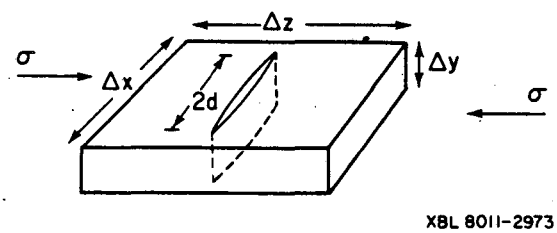

Figure 3. Typical geometry of a flat elliptic crack in rock block under stress.

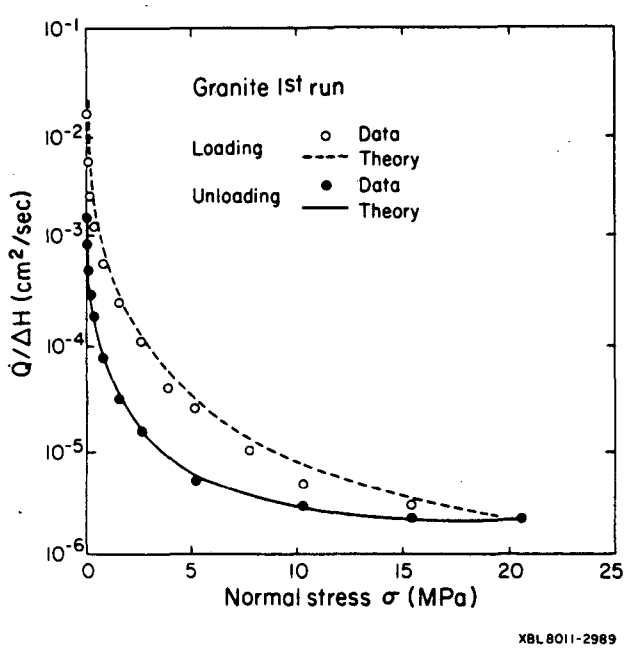

Figure 4. Flow as a function of normal stress in granite.

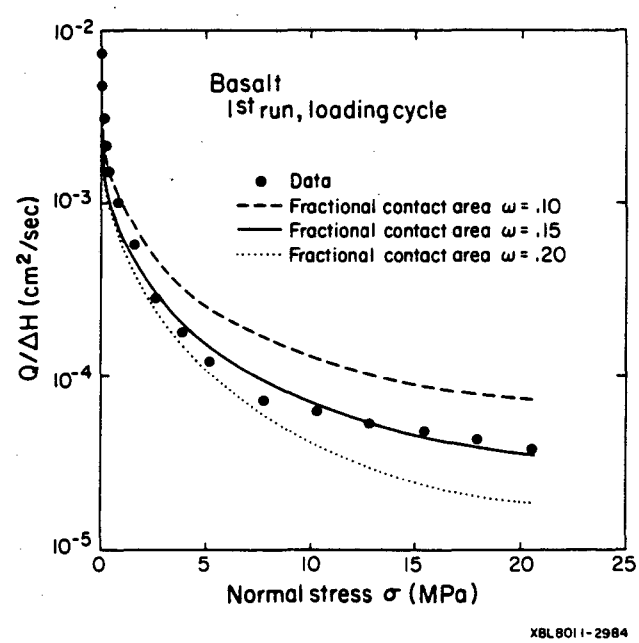

Figure 5. Flow as a function of normal stress in basalt.

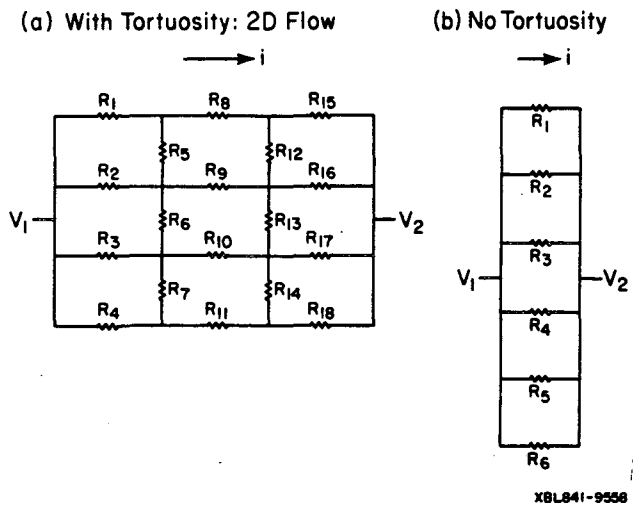

Figure 6. Electrical circuit equivalent of two-dimensional fluid flow (a) when tortuosity is present and (b) when tortuosity is absent.

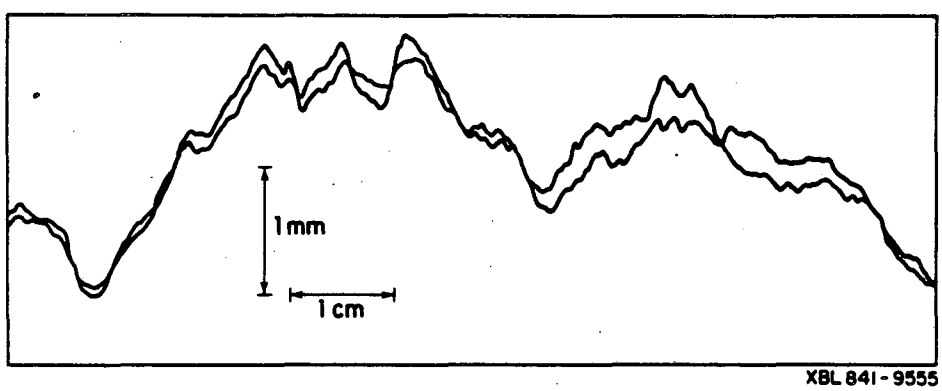

Figure 7. Surface roughness profiles of a granite fracture.

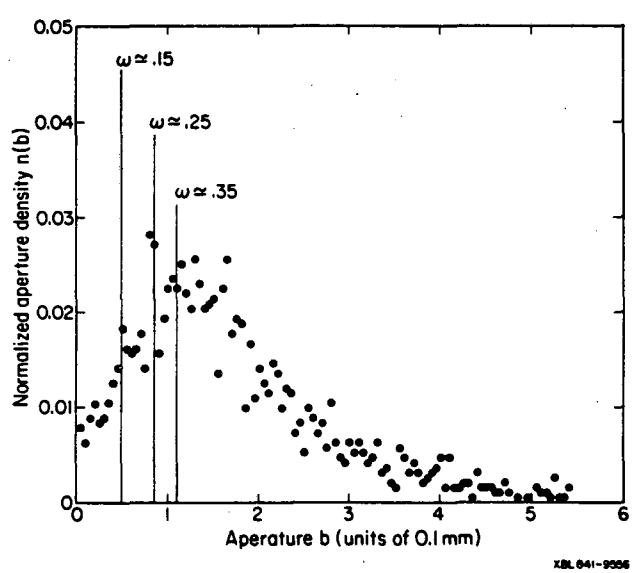

Figure 8. Aperture density distribution n(b) derived from ten sets of surface roughness profiles of a granite fracture.

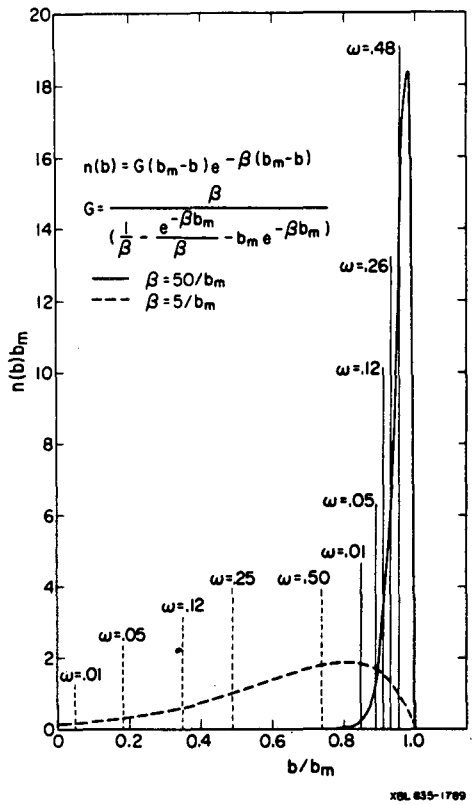

Figure 9. Skewed aperture distributions.

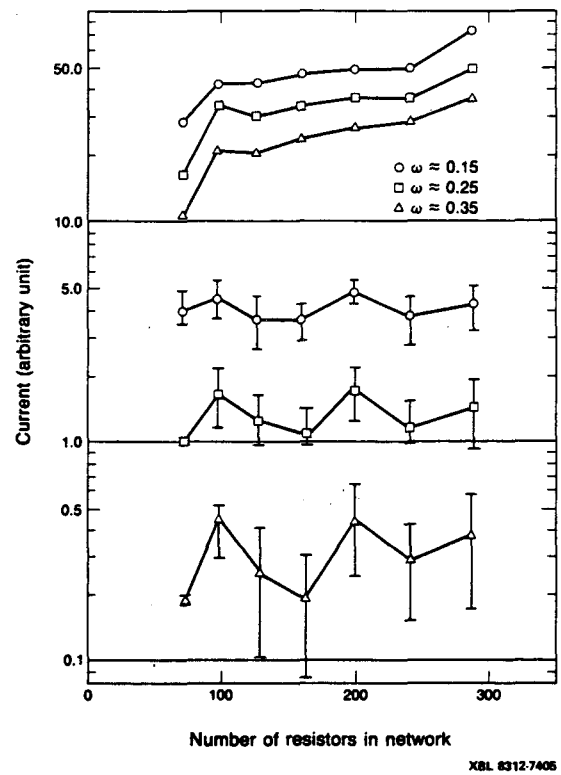

Figure 10. Calculated currents through resistances whose values are governed by the aperture density distributions in Figure 8.

This report was done with support from the Department of Energy. Any conclusions or opinions expressed in this report represent solely those of the author(s) and not necessarily those of The Regents of the University of California, the Lawrence Berkeley Laboratory or the Department of Energy.

Reference to a company or product name does not imply approval or recommendation of the product by the University of California or the U.S. Department of Energy to the exclusion of others that may be suitable.

TECHNICAL INFORMATION DEPARTMENT
LAWRENCE BERKELEY LABORATORY
UNIVERSITY OF CALIFORNIA
BERKELEY, CALIFORNIA 94720